Materials Science and Engineering B 165 (2009) 67–70

Contents lists available at ScienceDirect

Materials Science and Engineering B

journal homepage: www.elsevier.com/locate/mseb

Electrical characterisation of thin silicon layers by light beam induced current and internal quantum efficiency measurements

Y. Sayad [a], S. Amtablian [a], A. Kaminski [a,*], D. Blanc [a], P. Carroy [a], A. Nouiri [b], M. Lemiti [a]

[a] Institut de Nanotechnologies de Lyon, UMR - CNRS 5270, Site INSA - Lyon, Bât Blaise Pascal, 7 avenue Jean Capelle, 69621 Villeurbanne Cedex, France
[b] Institut de Physique, Université Mentouri, Route Ain El-Bay, 25000 Constantine, Algeria

ARTICLE INFO

Article history:
Received 18 June 2008
Received in revised form 17 February 2009
Accepted 4 April 2009

Keywords:
Diffusion length
LBIC
Quantum efficiency
Epitaxial silicon
Thin films
Solar cells

ABSTRACT

Thin crystalline silicon layers (50 μm) were grown by vapour phase epitaxy on monocrystalline substrates. Minority carrier diffusion length and surface recombination velocity were evaluated by light beam induced current experiment. Although it appeared difficult to apply existing analytical models to thin and high quality layers, multi-dimensional simulator DESSIS was used successfully to extract diffusion length of the order of 300 μm for p-type material and 80 μm for n-type material with surface recombination velocity of the order of 100–1000 cm s^{-1} when the surface was passivated by a thin silicon nitrite coating. Results were compared with the diffusion length evaluated from internal quantum efficiency analysis in fabricated photovoltaic cells made of the same material, using spectral response and reflectivity measurements.

1. Introduction

Since material represents an important part of the total photovoltaic module price [1], one way to reduce the cost is to fabricate silicon thin films. Layers of thickness 50 μm or less can be obtained by epitaxial growth which appears as a sustainable approach offering several advantages including high quality material, abrupt doping profile and in situ emitter formation that leads to a reduced thermal budget. Works on thin epitaxially grown layers are quite developed [2,3] and, combined with a layer transfer process [4], appears as a promising way to investigate. However, a critical factor for the success of thin film silicon solar cells is the electronic quality of the layer and the effect of the various processing steps on the efficiency of the final device. Accurate measurements of transport properties are therefore a major issue that still requires some improvements. In particular, the minority carrier diffusion length is one of the most important parameters affecting the solar cell performance that can be evaluated by light beam induced current (LBIC) and electron beam induced current (EBIC) in starting materials [5,6], or from internal quantum efficiency (IQE) [7–9] and *I–V* [10,11] measurements in complete solar cells.

This paper describes our first attempts at measuring minority carriers diffusion length on epitaxially grown thin films deposited on 4 in. crystalline substrates. Previous development of epitaxial silicon layers deposited on 2 in. substrates has permitted the fabrication of solar cells with a conversion efficiency $\eta = 9.5\%$ [12]. Since then, our reactor has been modified and experimental conditions (gas flux and temperature homogenisation) have been adapted to accommodate 4 in. substrates for larger area cells. Sample fabrication process is briefly explained, together with the two experimental techniques that have been used to extract the minority carrier diffusion length. Amongst available techniques, LBIC experiment appears as a non-destructive way of investigating the material quality with a high spatial resolution. Furthermore, spectrally resolved analysis of the quantum efficiency measured in solar cells brings complementary information on the bulk transport properties. A short review of the analytical models that have been developed in the past to relate material properties to experimental measurements is given and their limit of applicability in the case of thin and reasonably high quality material is pointed out. Numerical calculation is then used to give the best estimates of diffusion length and surface recombination velocities in our samples. Conclusions are finally drawn on the reliability of the characterisation techniques applied to thin solar cells.

2. Sample preparation

Crystalline silicon was elaborated by vapour phase epitaxy in an atmospheric pressure reactor (APCVD). The reactor has been developed in-house for silicon deposition on 4 in. wafers at a working temperature of 1100 °C. Growth rates between 0.3 μm/min and 2 μm/min are achievable. Dichlorosilane (SiH_2Cl_2) is used as the

* Corresponding author. Tel.: +33 472438540; fax: +33 472438531.
E-mail address: Anne.Kaminski@insa-lyon.fr (A. Kaminski).

0921-5107/$ – see front matter © 2009 Elsevier B.V. All rights reserved.
doi:10.1016/j.mseb.2009.04.007

silicon precursor in an hydrogen atmosphere and diborane (B_2H_6) and phosphine (PH_3) are respectively used for p-type and n-type doping. The 4 in. wafers are located on a SiC coated graphite holder which is heated by electromagnetic induction. The homogeneity of the epitaxial layer is ±1 μm on the whole wafer surface thanks to the sample rotation.

Samples for LBIC measurements were deposited at a growth rate of 1.2 μm/min on monocrystalline Cz heavily doped wafers. The thickness was 56 μm and the doping level was around $(5–7) \times 10^{16}$ at. cm^{-3}. The current collector was a Schottky contact made of a 25 nm semi-transparent evaporated chromium. The rear ohmic contact was taken with indium–gallium alloy applied on the silicon substrate back side. On some samples, a 75-nm thick SiN_x:H layer was deposited by PECVD, to reduce the surface recombination.

For spectral response measurements, a cell was fabricated with a p-type thin epitaxial layer (56 μm thick and $(5–7) \times 10^{16}$ at. cm^{-3} boron doped) deposited on a thick Cz type p^+ substrate (525 μm thick, $\rho = 0.01\ \Omega$ cm). Processing steps were the following: epitaxial growth, emitter formation by phosphorous diffusion with a sheet resistance of 67 Ω/□, antireflection coating and passivation by a 75-nm thick SiN_x:H, formation of the front contacts using a metallic alloy (Ti/Pd/Ag) and rear contact formation by aluminium deposition and annealing.

3. Light beam induced current (LBIC) analysis

LBIC experiment is based on the diffusion of the excess minority carriers that are generated in a p–n or a Schottky diode by a focused light beam. In our set-up, a laser diode (λ = 780 nm) is focused down to a 20 μm spot size diameter perpendicular to the sample surface. At this wavelength the penetration depth of the beam is of the order of 10 μm. The injection level is kept to a low level so that the majority carrier density is not significantly affected. The photo-induced current is measured as the beam is scanned away from the junction as shown in Fig. 1(a). A typical decay of the short-circuit current is represented in Fig. 1(b).

Analytical models have been developed in the past to extract the bulk diffusion length from the electron beam induced current

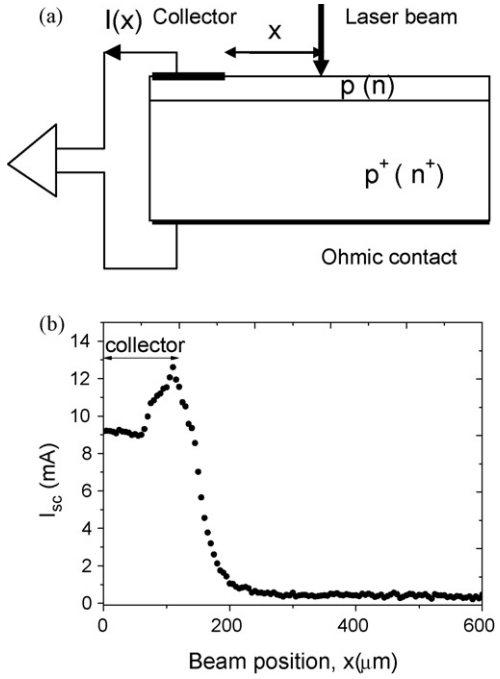

Fig. 1. (a) LBIC experimental set-up and (b) typical LBIC signal.

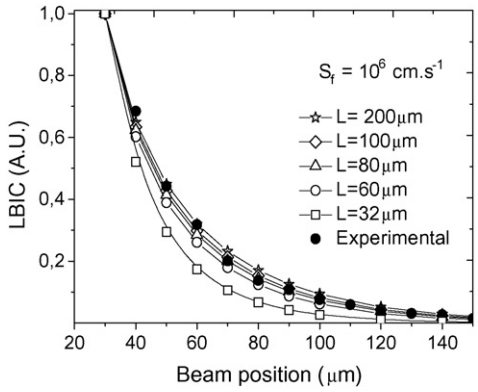

Fig. 2. Experimental (scattered points) and calculated (solid lines and symbols) LBIC for p-type non-passivated sample.

(EBIC) experiments [5,13–15] and have been extended to the case of light beam illumination [16,17]. These models are attractive because they are based on physical considerations (quasi-exponential decay of the photo-induced current) and lead to approximate analytical solutions of the form (1) first proposed to describe the decay of the EBIC current in thick semiconductors [6]:

$$\mathrm{LBIC}(x) = C \exp\left(-\frac{x}{L}\right) \cdot x^{-n} \quad (1)$$

where L is the minority carriers diffusion length, C is a constant proportional to signal amplitude and depending on photons flux, wavelength, reflectivity and beam size and n takes into account the surface recombination velocity S_f on the front surface (n varies between 0.5 and 1.5 when S_f increases from 0 to ∞). This expression has been used successfully in our group to deduce diffusion length of the order of 20–50 μm in 200 μm thick multicrystalline samples (POLIX) [17]. However, difficulties arise in the case of thin samples, in particular when the surface plays a major role in recombination mechanisms.

The applicability of Eq. (1) was verified by simulations of the photocurrent as a function of the ratio W/L where W is the sample thickness. For numerical simulation, the software DESSIS, part of the modelling tool pack ISE TCAD 8.5 was used. It relies on advanced physical models and numerical methods for 2D simulation of semiconductor devices. Recombination, mobility and doping-dependant lifetime models as defined in [18] were used. Monochromatic incident beam was defined with a wavelength of 780 nm. Theoretical photocurrent decays were calculated with imposed parameters (front surface recombination velocity S_f, back surface recombination velocity S_b, L and W) and the resulting curves were fitted with Eq. (1) to try and determine the fitted value of L and n. Other user defined parameters were the light beam wavelength (780 nm), size and intensity. It was found that Eq. (1) could only be applied to extract L when $W \geq 4L$ independently of S_f and S_b. Surface recombination influences the n parameter only, which varies from 0.34 to 1.25 when surface recombination velocity varies between 10^2 and 10^6 cm s^{-1}.

As expected from the above discussion, Eq. (1) could not be applied to evaluate the diffusion length from the experimental curves measured on thin samples ($W \leq 4L$). Therefore, a theoretical LBIC profile was calculated numerically with the software DESSIS using the experimental parameters (spot size, wavelength of incident laser beam, doping concentration). Results are presented for the case of p-type silicon but similar results are obtained for n-type layers. The simulated curves (Fig. 2) show that if the front surface recombination velocity is large ($S_f \geq 10^6$ cm s^{-1}), the diffusion length cannot be evaluated precisely, except for low diffusion length values. Indeed, for $S_f = 10^6$ cm s^{-1} and $L \geq 60$ μm the curves

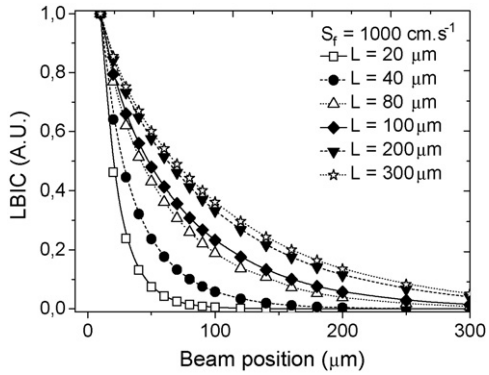

Fig. 3. Calculated LBIC decays for $S_f = 1000\,\mathrm{cm\,s^{-1}}$ (passivated front surface) and different diffusion length values (p-type passivated sample).

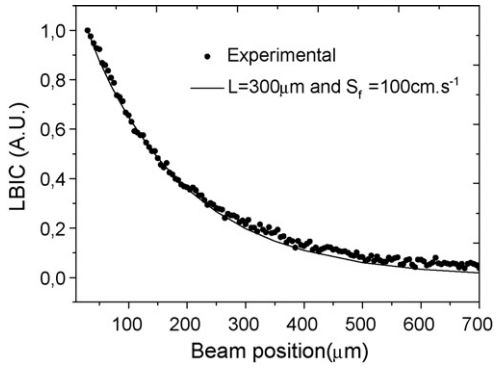

Fig. 4. Experimental and best-fit LBIC curves for surface passivated p-type sample.

are superimposed, indicating that the photocurrent decay is dominated by surface recombination. Therefore, in the case of high surface recombination velocities, only a lower limit of the diffusion length can be estimated ($L > 60\,\mu\mathrm{m}$).

On the other hand, when the surface recombination velocity is relatively low ($S_f = 10^3\,\mathrm{cm\,s^{-1}}$, for example), the diffusion length of the minority carriers dominates the current decay and it can be reasonably well evaluated from the shape of the photocurrent decay (Fig. 3).

To satisfy the condition of low S_f values, the front surface of p- and n-type samples was coated with a SiN_x:H layer that is known to passivate defects [19]. Experimental results and theoretical curves are presented in Figs. 4 and 5. For the p-type layer, optimised fitting parameters are $S_f \approx 100\,\mathrm{cm\,s^{-1}}$ and $L \approx 300\,\mu\mathrm{m}$ while for n-type samples fitting parameters were $S_f \approx 2000\,\mathrm{cm\,s^{-1}}$ and $L \approx 80\,\mu\mathrm{m}$. These results agree reasonably well with expected values.

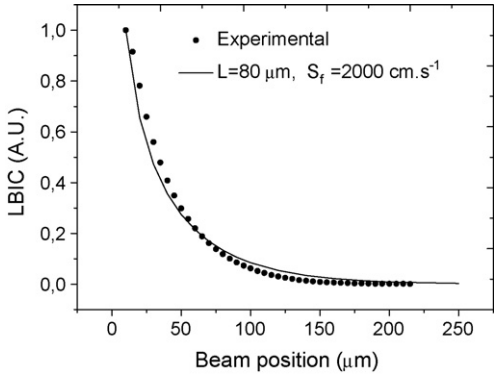

Fig. 5. Experimental and best-fit LBIC curves for surface passivated n-type sample.

4. Quantum efficiency analysis

Quantum efficiency analysis is commonly used to gain information on the bulk diffusion length of minority carriers and on the back surface recombination velocity. It gives the fraction of carriers generated by the solar cell compared to the number of photons incident on the device. Quantum efficiency is directly related to the spectral response which is measured experimentally as the ratio of the current generated by the solar cell I_{sc} to the power incident on the solar cell P_{in}, as expressed by Eq. (2):

$$\mathrm{SR}(\lambda) = \frac{I_{sc}(\lambda)}{P_{in}(\lambda)} \tag{2}$$

Using a calibrated cell one deduces directly the external quantum efficiency EQE related to the spectral response SR(λ) by Eq. (3):

$$\mathrm{EQE}(\lambda) = \mathrm{SR}(\lambda) \cdot \frac{hc}{q\lambda} \tag{3}$$

where h is the Planck constant, c the speed of light in vacuum, q the elementary charge of an electron and λ is the wavelength of the incident light.

After spectral reflectivity $R(\lambda)$ measurements the internal quantum efficiency IQE (Fig. 8) can be expressed as a function of wavelength:

$$\mathrm{IQE}(\lambda) = \frac{\mathrm{EQE}(\lambda)}{1 - R(\lambda)} \tag{4}$$

In thick standard solar cells when neglecting the emitter and the space charge region contributions for wavelengths ($\lambda > 800\,\mathrm{nm}$) satisfying $\alpha W \gg 1$ (α is the absorption coefficient) and when neglecting the back surface internal reflectivity for near-infrared region ($800\,\mathrm{nm} < \lambda < 1000\,\mathrm{nm}$), a linear relationship can be written between the inverse of the IQE and the penetration depth (α^{-1}) [7,8]:

$$\frac{1}{\mathrm{IQE}} = 1 + \frac{1}{L_{\mathrm{eff}}}\left(\frac{1}{\alpha}\right) \tag{5}$$

where L_{eff} is an effective diffusion length expressed by

$$L_{\mathrm{eff}} = L_b \left\{ \frac{(S_b L_b/D) + \tanh(W/L_b)}{1 + (S_b L_b/D)\tanh(W/L_b)} \right\} \tag{6}$$

W is the cell thickness, S_b, L_b and D represent the recombination velocity at the back surface, the diffusion length in the base region and the diffusion coefficient of the minority carriers respectively. The above expression was extended to obtain more accurate determination of the diffusion length and the following expression of IQE was proposed [9]:

$$\mathrm{IQE} \approx e^{-d} \frac{1 - (\alpha L_{\mathrm{eff}})^{-1}}{1 - (\alpha \cdot L_b)^{-2}} \tag{7}$$

where d is the thickness of the emitter. Eq. (7) is valid for wavelengths that verify the two following conditions: (i) $1/\alpha > 14\,\mu\mathrm{m}$ (equivalent to $\lambda \geq 820\,\mathrm{nm}$) and (ii) $1/\alpha < W/4$. From the above conditions, it appears that in presence of a rear thick p^+ substrate where the internal reflectivity on back surface can be neglected, there is no longer an upper wavelength limit for the applicability of Eqs. (5) and (7).

Experimental internal quantum efficiency data are plotted in Figs. 6 and 7 versus $1/\alpha$ and α respectively, together with the fitted curves corresponding to analytical expressions (5) and (7) respectively. The extracted value of L_{eff} ($=L_b$) is 32 μm. The discrepancies between experimental and theoretical curves for low values of $1/\alpha$ (and λ) can be explained by the small contribution of the emitter and of the space charge region to IQE (this contribution has been neglected in formulas (5) and (7)).

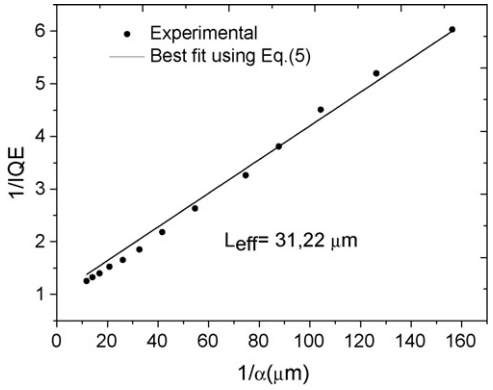

Fig. 6. Experimental inverse internal quantum efficiency versus light penetration depth and best fit using Eq. (5).

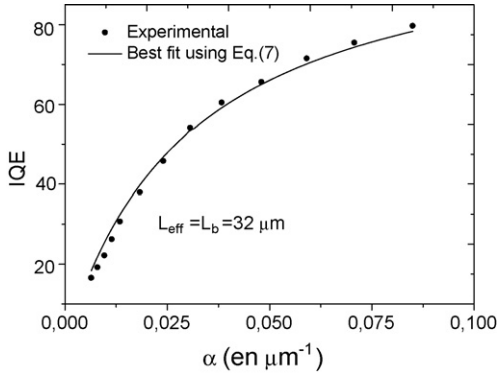

Fig. 7. Internal quantum efficiency versus absorption coefficient, and fit by Eq. (7).

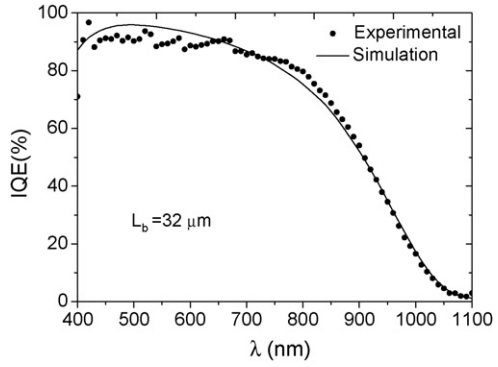

Fig. 8. Internal quantum efficiency versus wavelength and simulated curve using PC1D software.

We have also tried to fit directly experimental IQE curves with the 1D PC1D software [20]. This 1D software permits to calculate solar cells *I–V* characteristics, as well as EQE and IQE. We have varied L_b value in the parameters used to simulate the solar cell in order to obtain the best fit. Finally, the best fit is obtained for $L_b = 32\ \mu m$ (Fig. 8) confirming previous extraction with analytical expressions (5) and (7).

L_b value determined on finished solar cells is very low compared to the one obtained by LBIC analysis. The discrepancy can be explained by the fact that LBIC is a very local measurement (spot size of the order of 20 μm diameter) performed on the material before processing, while in IQE analysis, the photocurrent is averaged over a spot size of 9 mm^2 on the solar cell. IQE measurements suggest that the epitaxial layer is not homogeneous over large areas (presence of defects in the epitaxial layer) and that high temperature processing may degrade the material quality during solar cell elaboration.

5. Conclusion

Good quality 50 μm thick crystalline silicon layer were elaborated by vapour phase epitaxy and solar cells were fabricated using standard processes. It was shown that analytical models that describe minority carriers diffusion in monocrystalline silicon wafers were not usually applicable to the case of thin layers. However, fitting procedures were used successfully to get an estimate of carrier diffusion length and surface recombination velocity in thin crystalline layers. LBIC measurements showed that when the surface recombination is sufficiently low (i.e. for a front surface passivated with SiN_x:H), the diffusion length of minority carriers in a p-type layer with a doping concentration of $(5–7) \times 10^{16}$ at cm^{-3} was close to 300 μm. Similarly, diffusion length of minority carriers in n-type samples was found to be around 80 μm. IQE analysis appeared as a way to assess the homogeneity of the starting material and the effect of the processing steps on the final solar cell.

Acknowledgements

The first author gratefully acknowledges the Comité Mixte d'Evaluation Prospective (CMEP) de la Cooperation Inter-universitaire franco-Algérienne for financial support. This work has been supported by ANR, the French national research agency and by ADEME, the French Agency for Environment and Energy Management.

References

[1] A. Müller, M. Ghosh, R. Sonnenschein, P. Woditsch, Material Science and Engineering B 134 (2006) 257.
[2] E. Schmich, N. Schillinger, S. Reber, Surface and Coatings Technology 201 (2007) 9325.
[3] T. Kunz, I. Burkert, R. Auer, A.A. Lovtsus, R.A. Talalaev, Yu.N. Makarov, Journal of Crystal Growth 310 (6) (2008) 1112.
[4] J. Kraiem, S. Amtablian, O. Nichiporuk, P. Papet, J.-F. Lelievre, A. Fave, A. Kaminiski, P.-J. Ribeyron, M. Lemiti, Proc. 21st Eu. Photovolt. Solar Energy Conf., Dresden, 2006, p. 1268.
[5] S.M. Davidson, C.A. Dimitriadis, Journal of Microscopy 118 (Pt. 3) (1980) 275.
[6] K. Masri, J.P. Boyeaux, D. Sarti, L. Mayet, S.N. Kumar, A. Laugier, Proc. 9th Eu. Photovolt. Solar Energy Conf., Freiburg, 1989, p. 620.
[7] P.A. Basore, Proc. 23rd IEEE Photovolt. Spec. Conf., 1993, p. 147.
[8] S. Keller, M. Spiegel, P. Fath, G.P. Willeke, E. Bucher, IEEE Transaction of Electron Devices 45 (July) (1998) 1569.
[9] M. Spiegel, B. Fischer, S. Keller, E. Bucher, Proc. 28th IEEE Photovolt. Spec. Conf., 2000, p. 311.
[10] U. Taretto, J.H. Rau, Werner, Journal of Applied Physics 93 (9) (2003) 5447.
[11] J.M. Zhu, W.Z. Shen, Y.H. Zhang, H.F.W. Dekkers, Physica B 355 (2005) 408.
[12] S. Amtablian, D. Eon, A. Kaminski, A. Fave, P. Roca i Cabarrocas, P.-J. Ribeyron, M. Lemiti, Proc. 22nd Eu. Photovolt. Solar Energy Conf., September 2007, p. 1990.
[13] H. Holloway, Journal of Applied Physics 55 (10) (1984) 3669.
[14] Th. Flohr, R. Helbig, Journal of Applied Physics 66 (7) (1989) 3060.
[15] D.E. Ioannou, C.A. Dimitriadis, IEEE Transactions of Electron Devices ED-29 (3) (1982) 445.
[16] D.E. Ioannou, R.J. Gledhill, IEEE Transactions Electron Devices ED-30 (6) (1983) 577.
[17] J.P. Boyeaux, A. Laugier, Revue de Physique Appliquée, Colloque C6, Supplément au No. 6, Tome 24, 1989, p. 111.
[18] O. Nichiporuk, A. Kaminski, M. Lemiti, A. Fave, V. Skryshevsky, Solar Energy Materials and Solar Cell 86 (2005) 517.
[19] J.-F. Lelièvre, E. Fourmond, A. Kaminski, M. Lemiti, O. Palais, D. Ballutaud, Solar Energy Materials and Solar Cells, in press.
[20] D.A. Clugston, P.A. Basore, Proc. 26th IEEE Photovolt. Spec. Conf., September 1997, p. 207.